

DOI: 10.24850/j-tyca-2024-06-04

Articles

## **Analysis and risk prevention of flooding in high-risk gorges in the city of Arequipa, Peru**

### **Análisis y prevención del peligro por inundaciones en quebradas de alto riesgo en la ciudad de Arequipa, Perú**

Joel Ccancapa-Puma<sup>1</sup>, ORCID: <https://orcid.org/0009-0005-4439-0711>

Alejandro Víctor Hidalgo-Valdivia<sup>2</sup>, ORCID: <https://orcid.org/0000-0002-7598-9074>

Guillermo Yorel Noriega-Aquise<sup>3</sup>, ORCID: <https://orcid.org/0000-0003-2354-6391>

Alex Eduardo Aguilar-Chávez<sup>4</sup>, ORCID: <https://orcid.org/0000-0003-4982-5671>

Marcelo Marques<sup>5</sup>, ORCID: <https://orcid.org/0000-0001-5451-5323>

<sup>1</sup>Universidad Católica de Santa María (UCSM), Escuela Profesional de Ingeniería Civil, Arequipa, Perú, [joel.ccancapa@ucsm.edu.pe](mailto:joel.ccancapa@ucsm.edu.pe)

<sup>2</sup>Universidad Católica de Santa María (UCSM), Escuela Profesional de Ingeniería Civil, Arequipa, Perú, [ahidalgo@ucsm.edu.pe](mailto:ahidalgo@ucsm.edu.pe)

<sup>3</sup>Iniversidad Católica de Santa María (UCSM), Escuela Profesional de Ingeniería Civil, Arequipa, Perú, [gnoriega@ucsm.edu.pe](mailto:gnoriega@ucsm.edu.pe)



<sup>4</sup>Universidad Católica de Santa María (UCSM), Escuela Profesional de Ingeniería Civil, Arequipa, Perú, aaguilarch@ucsm.edu.pe

<sup>5</sup>Universidad Estadual de Maringá (UEM), Umuarama, Brasil, mmarques@uem.br

Corresponding author: Joel Ccancapa-Puma,  
joel.ccancapa@ucsm.edu.pe

## Abstract

The city of Arequipa, the second most important city in Perú, faces numerous daunting challenges, including high-intensity but short-in-duration rainfalls that leads to floods and the swelling of the Chili River (mud and landslides). This situation aggravates the vulnerability of the population settled on the margins of the gorges and gullies, due to little or no territorial planning from public institutions. The local news evidence negligence every year, both in terms of human lives and infrastructure loss. The frequency of these events has increased with time and that is the reason for prompting the establishment of rainfall thresholds and the compilation of a 41-year record (1981-2021), with the aim of informing about the dangerousness of an adverse meteorological phenomenon, either predicted or in progress. For the hydrological model, the authors used the highest 24-hour precipitation data from the SENAMHI's stations (National Service of Meteorology and Hydrology of Peru) to generate the liquid hydrograph for different return periods with the Hydrologic model of HEC-HMS. Soil mechanics studies were also carried out to determine



the rheological parameters of the non-Newtonian flow and then calibrate through historical events in a hydraulic model of HEC-RAS. Finally, cartographic maps in QGIS were prepared to evaluate the hazard zones flooding in the Del Pato, San Lázaro, Venezuela and Los Incas gullies.

**Keywords:** Extreme events, rainfall thresholds, hyper-concentrated flows, floods, hazard, Arequipa.

## Resumen

La ciudad de Arequipa, la segunda ciudad más importante del Perú, enfrenta eventos extremos, como lluvias de alta intensidad, pero de corta duración, que generan inundaciones y crecidas del río Chili (avenidas de lodo y huaycos). Esta situación agrava la vulnerabilidad de la población asentada en las márgenes de las quebradas, posteriormente torreneras, debido a la poca o nula planificación territorial por parte de las entidades gubernamentales, que se refleja cada año en pérdidas humanas y de infraestructura. La frecuencia de estos eventos va en aumento con el tiempo y es por esta razón que se generan umbrales de precipitaciones extremas para su correspondiente caracterización, con un registro de 41 años (1981-2021), a fin de informar sobre la peligrosidad de un fenómeno meteorológico adverso, previsto o en desarrollo. Se utilizaron datos de precipitación máxima de 24 horas de las estaciones meteorológicas del Servicio Nacional de Meteorología e Hidrología del Perú (SENAMHI) para obtener el hidrograma líquido para diferentes períodos de retorno con el modelo hidrológico HEC-HMS. También se realizaron estudios de mecánica de suelos para determinar los parámetros reológicos del flujo no newtoniano y luego calibrar a través de eventos históricos con el



modelo hidráulico HEC-RAS. Finalmente se elaboraron mapas cartográficos en QGIS para evaluar las zonas de peligro por inundaciones en las torreteras Del Pato, San Lázaro, Venezuela y Los Incas.

**Palabras clave:** eventos extremos, umbrales de precipitación, flujos hiperconcentrados, inundaciones, peligro, Arequipa.

Received: 29/03/2023

Accepted: 07/07/2023

Published Online: 21/07/2023

## Introduction

Perú is highly exposed to climate change, which affects the severity and occurrence of meteorological phenomena such as El Niño (Espinoza-Vigil & Booker, 2023a), a situation that is aggravated by the situation of inequality, poverty and population growth (IPCC, 2022).

Arequipa, is home to more than 1 million 316 thousand inhabitants according to the National Institute of Statistics and Informatics of Peru (INEI, 2017).

The city of Arequipa suffers from overflows and floods every year in areas adjacent to the channels of the gully that enter and converge in the Chili River, collapsing sewers and areas of cultivated area settled in the lower areas of the Misti volcano, since that short-term but high-intensity rainfall occurs, in such a way that, in the last 20 years, extreme storms have become increasingly frequent due to climate change, triggering



more critical flows into existing gullies. These extreme rains have evidenced the poor dimensioning and destruction of the bridges over the gullies and riverbeds (Espinoza-Vigil & Booker, 2023b), as well as inadequate urban planning (El Búho, 2021).

A basic indicator for adequate planning and programming of economic, socio-economic, socio-environmental and territorial intervention activities is to understanding the different climatic regimes. The National Meteorology and Hydrology Service of Peru [SENAMHI] in 2020 produced the report Climates of Peru: National Climate Classification Map and it was updated in 2021 by the Thornthwaite method, as a tool to know the different types of climate in Peru, for decision-making and disaster risk reduction, prevailing in the city of Arequipa an arid and temperate climate **E(d)B'** with moisture deficiency in all seasons of the year (SENAMHI, 2021).

The National Water Authority [ANA], as the governing body of the national water resources management system, produced a report called Prioritization of Basins for Water Resources Management (ANA, 2016), with the aim of ensuring continuity through a sustainable and responsible development of water resources, based on criteria and indicators, one of these indicators establishes that the Quilca-Chili basin, as the most vulnerable, considered high priority (at the first level) predominating the hydrological aspect (Water Stress), as well as the presence of critical points in the face of extreme events (Floods) (ANA, 2015).

Extreme events in the city of Arequipa trigger floods associated with fluvial erosion processes, where their erosive force is often caused by sediment load (mud flows or debris). According to Vílchez & Sosa (2021),

these conditions in the Del Pato, San Lázaro, Venezuela and Los Incas gullies mean that there is a high risk of flooding and fluvial erosion (Figure 1), according to the heuristic qualitative.



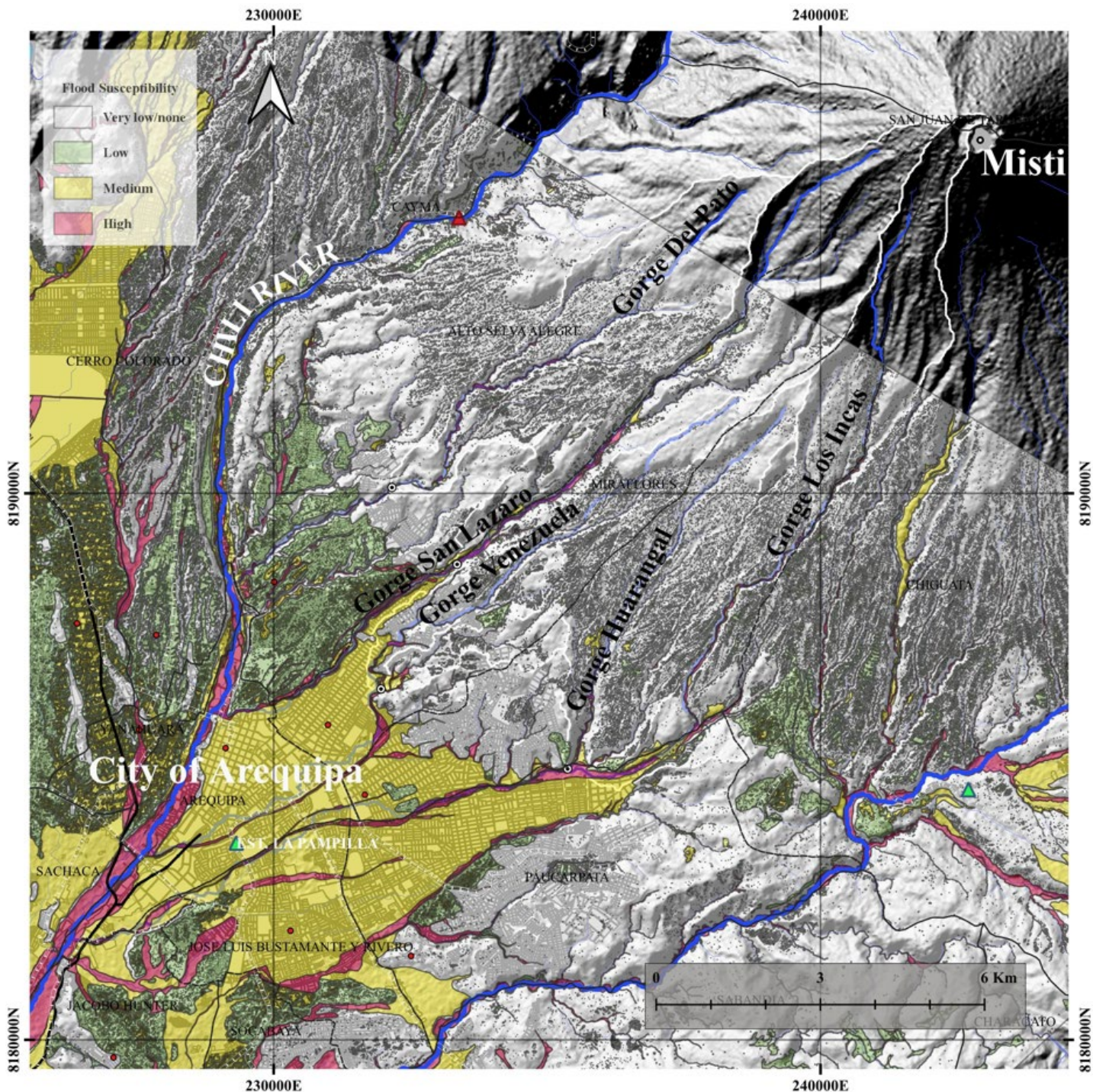


**Figure 1.** Data base adaptation from Flood and Fluvial Erosion Susceptibility. Source: Vílchez and Sosa (2021).

United Nations (2014) defines "danger" as the degree of threat to places or human settlements due to unfavorable phenomena in a given period of time.

The latest report from the World Economic Forum (2023) on global risks, has identified by severity in the short and long term that natural disasters and extreme weather events are the most critical, for which we are less and less prepared for the impacts of climate change.

Due to historical events during the rainy season (January, February and March) that occur each year in the city of Arequipa, this study has the general objective of characterizing the extreme rainfall recorded by the La Pampilla station through maximum precipitation thresholds, in order to report the danger of an adverse meteorological phenomenon, predicted or in development, thus constituting a climatic index of extreme rainfall, with a practical and internationally recognized method.

The occurrence of floods in magnitude and frequency for water resources management is of vital importance, therefore, as specific objectives, topographic, geotechnical, hydrological and hydraulic studies were carried out in the evaluated gullies to understand the behavior of the basins and mitigate the impact.

## Materials and methods

The city of Arequipa (Figure 2) is severely affected with irregular periodicity to floods due to the activation of the gullies on the right and left side of the Chili river bank. According to the diagnosis presented by the ANA (2015) called the Water Resources Management Plan of the Cuenca Quilca-Chili the city, is the point of greatest risk for landslides, mainly due to the indiscriminate growth of the city due to a lack of planning, a poor sewage system and the invasion of natural channels. The city of Arequipa has an area of 676.6 km<sup>2</sup>, it is located within the Quilca-Chili basin with an area of 13,457 km<sup>2</sup> and is located on the western slope of the Andes mountain range, which is why it belongs to the slope of the Pacific Ocean. It covers practically the entire province of Arequipa, to the southwest of Peruvian territory, between South Latitude 15° 37' 50" and 16° 47' 10" and West Longitude 70° 49' 15" and 72° 26' 35".

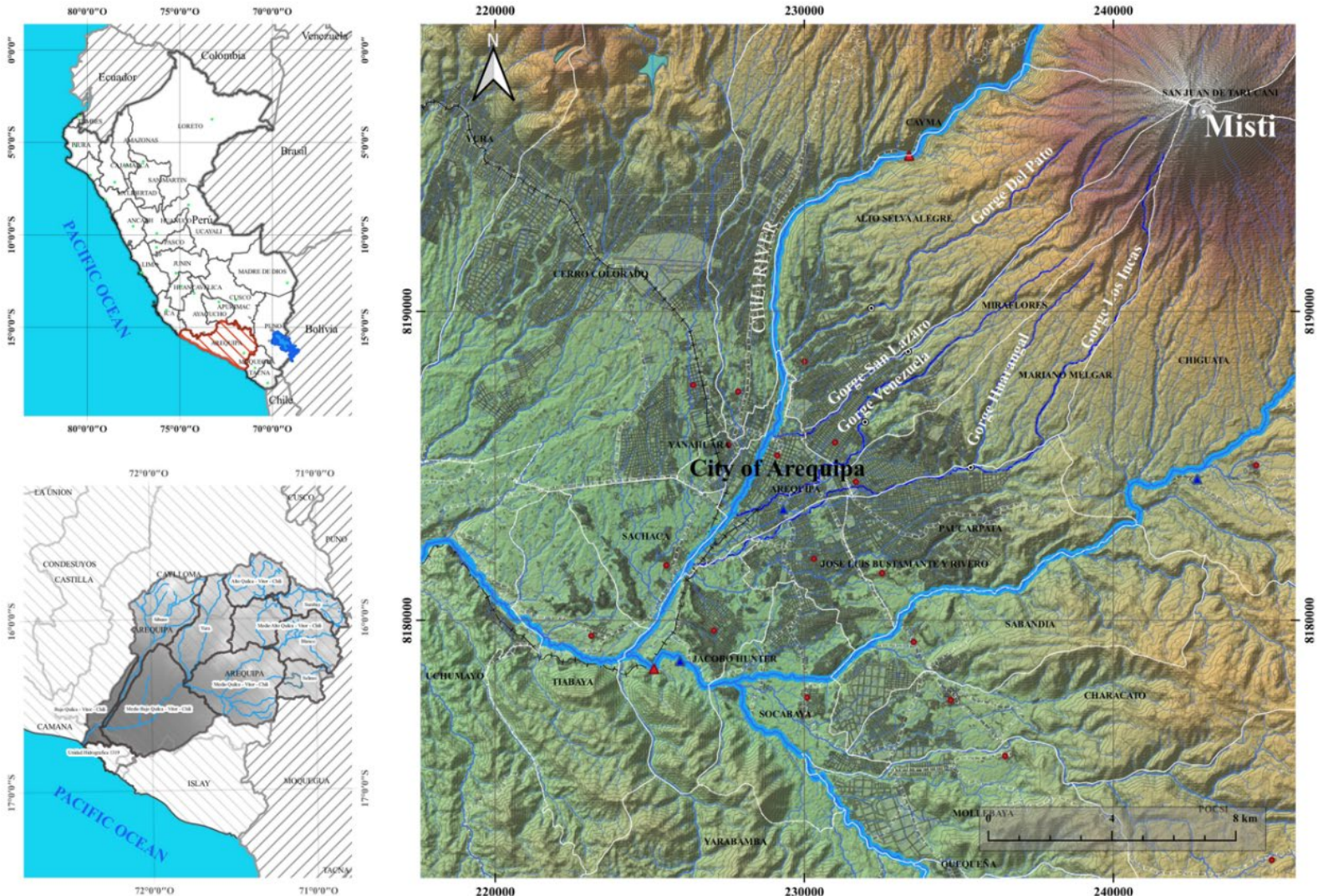


**Figure 2.** Location of the city of Arequipa and gullies under the Misti volcano.

Next, information on historical events that occurred in the city of Arequipa (1989-2021) was collected through articles, newspapers and institutions such as: ANA, SENAMHI and INGEMMET (Geological, Mining and Metallurgical Institute).

- **1989:** February 8, there was intense rain (37.7 mm/h) that caused all the gullies to activate, causing the flow of the Chili River to increase.
- **1997:** February 25, due to heavy rains, the San Lázaro, Miraflores, Paucarpata and Mariano Melgar streams overflowed, affecting Alto Selva Alegre, P.J. Ciudad Blanca – Comité and Cercado of Arequipa. It caused the death of 05 people and many damages.
- **2000:** January 18, intense rains caused the flooding of human settlements El Mirador, Pueblo Libre, Los Ángeles and Villa María del Triunfo (Mariano Melgar district). January 20, houses flooded by rain (Paucarpata district).
- **2001:** March 19, Heavy rains caused flooding in Cayma, Paucarpata, Socabaya, Alto Selva Alegre, José Luis Bustamante and Rivero. March 20, Floods in Alto Selva Alegre and Arequipa.
- **2008:** January 9, heavy rains in the districts of Alto Selva Alegre, Cayma, Hunter and Mariano Melgar.
- **2012:** January 1, heavy rains in the Alto Selva Alegre district.
- **2013:** February 8, intense rains (124.5 mm) originated that concentrated in the headwaters of the San Lázaro, Venezuela and Los Incas gullies. Material dragged downstream as debris flows, after 04 intense hours of precipitation. These flows affected tracks, homes, public and private infrastructure, and also caused the death of people.
- **2015:** January 1, Arequipa flood after 6 hours of rain.
- **2016:** January 26, Floods in the districts of Paucarpata, José Luis Bustamante and Rivero, Alto Selva Alegre.

- **2017:** January 13, in Alto Selva Alegre, the sectors of Villa Ecológica Independencia and Las Gardenias were affected, 150 houses affected by the landslides.
- **2020:** February 26, heavy rains affected more than 250 homes due to flooding in 6 districts, mudflow at the bus terminal and Terrapuerto (Figure 3, Figure 4, Figure 5, Figure 6, Figure 7, Figure 8, Figure 9).

(A)



(B)



**Figure 3.** Record of February 8, 1989. A), B) Recorded overflow of the Chili River, as a consequence of the construction of the Bajo Grau bridge that served as a dam, diverting the flow of water through the working-class neighborhood. Source: Climate and Ecology of Arequipa (2013).

(A)



(B)



(C)



(D)



**Figure 4.** Record of February 8, 2012. A), B) Flooding of the Chili river shows the vulnerability of the Bajo Grau Bridge. C), D) heavy rains are observed in the main streets Puente Grau and Bolívar. Source: Villalobos (2012).

(A)



(B)



(C)



(D)



**Figure 5.** Flood recorded on February 8, 2013 in the city of Arequipa.

A), B) Streets invaded by mud due to the activation of gorges later gullies. C), D) Destroyed roads as a consequence of the flooding caused by the heavy rain recorded. Source: Diario Correo (2014).

(A)



(B)



(C)



**Figure 6.** Record of February 2 and 29, 2015. A) Homes were damaged by torrential rains. B) Flooding of the road interchange of the Uchumayo variant. C) Heavy rains reveal the precariousness of road works. Source: El Búho (2015a; 2015b; 2015c)).



**Figure 7.** Record of February 23 and 24, 2016. A) 10-hour rain affected the city of Arequipa and the collapse of several transformers that left without electricity in several districts. B) The intense rains that occurred damaged infrastructures, urban roads and the entry of mudflows to houses settled on the banks of streams. Source: El Búho (2016a; 2016b).

(A)



(B)



**Figure 8.** Record of March 8 and January 30, 2017. A) Collapse of the Concordia Bridge in the Chulo stream due to heavy rains that affected the city of Arequipa. B) Heavy rains triggered the activation of the Paucarpata gorge, producing landslides . Source: El Búho (2017a; 2017b)).



**Figure 9.** Record of February 25 and 26, 2020. A), B) Heavy rainfall was recorded, causing the activation of gorges and landslides that swept away vehicles and flooded homes. C), D) Significant damages in six districts, more than 350 houses have been affected as a result of the floods and overflow of the gullies and entry of mud to the bus terminal and Terrapuerto of the city of Arequipa. Source: El Búho (2020a; 2020b; 2020c; 202d)).

## Basic studies

To understand the occurrence of floods, this study proposes a methodology based on basic studies such as topography, soil mechanical hydrology, and hydraulics in Del Pato, San Lázaro, Venezuela and Los Incas gullies of the city of Arequipa, to characterize the behavior of heavy rains and that aggravate the situation when they reach significant values (99th percentile), causing economic losses that exceed S/ 350 million and more than 80 thousand people affected by torrential rains (Gestion, 2013).

## Geology

The displacement or removal of rock masses (fractured and/or weathered), unconsolidated deposits or both due to the effect of gravity, are closely linked to intense rains, earthquakes and anthropic modifications (triggering factors), which also respond to conditioning or intrinsic factors, such as slope, morphology, vegetation cover, etc. (Vílchez & Sosa, 2021). The lithological characterization carried out by identified units and subunits of unconsolidated fluvial (**I-2**), alluvial (**I-3**), proluvial (**I-4**), colluvial (**I-6**), lacustrine (**I-7**), glacier (**I-8**) and volcanoclastic (**I-9**) deposits, as conditioning factors to mass movement. Ettinger *et al.* (2015) also mention that flash floods are common in semi-arid areas, such as Arequipa, where heavy rains occur annually between the months of January, February and March, having devastating effects in terms of geomorphology and human lives.

According to the Ministry of the Environment (MINAM, 2018), the city of Arequipa presents to the northeast volcanic flows from the Chachani and Misti (**NpQ-ba-s**) cut by the Chili river canyon, the city and surroundings correspond to fan deposits alluvial (**Qp-al**), to the west by volcanic tuffs, to the east by mudflow and to the south by the batholith of the caldera (Figure 10).

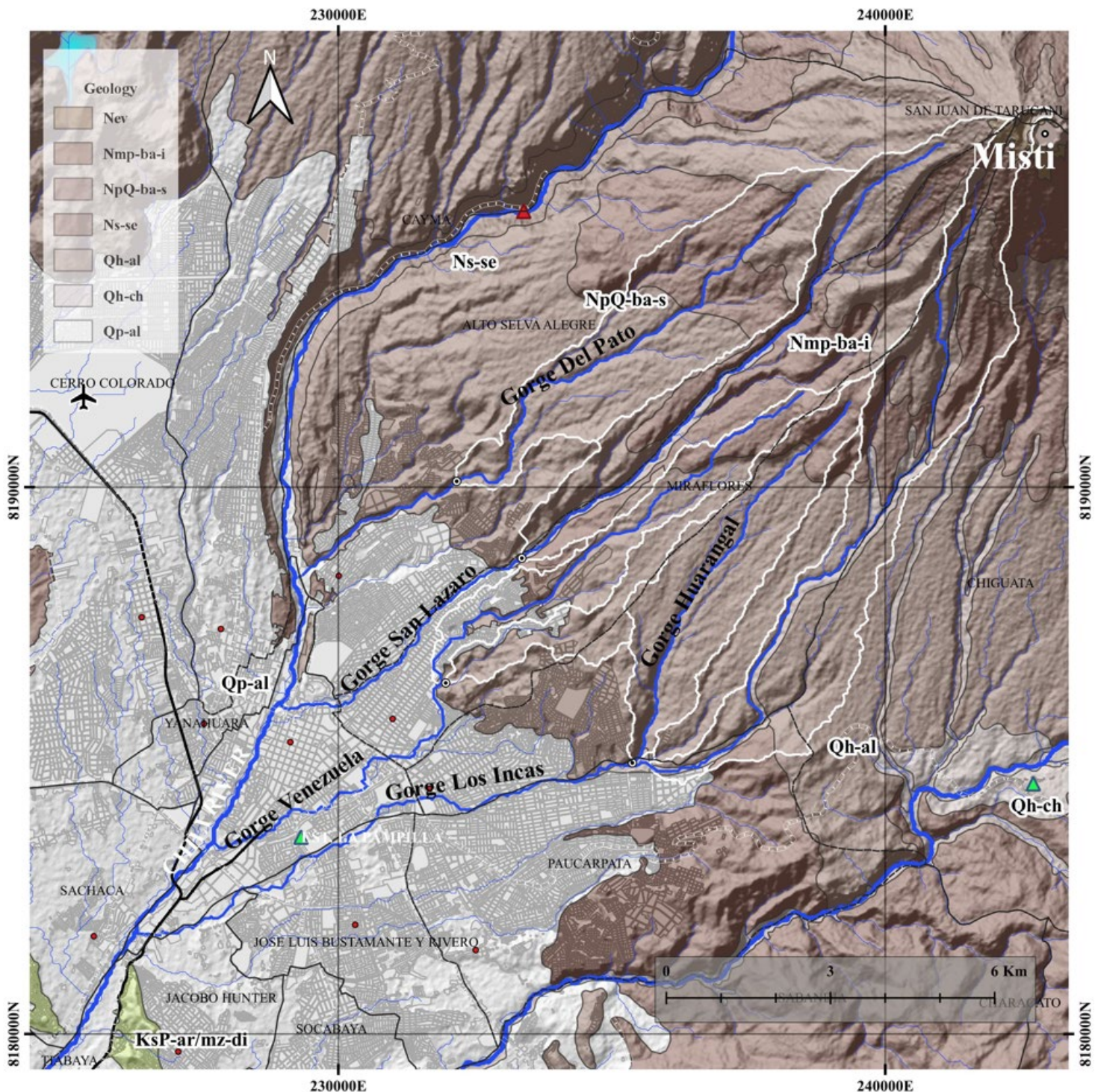


**Figure 10.** Geology database adaptation, MINAM (2018).

## Topography

The topographic survey of the main gullies was carried out using a DJI Phantom 4 RTK drone using the photogrammetry method, due to the high precision it offers due to stereoscopic vision and differential GPS. Obtaining contour lines every meter, georeferenced from a control point provided by the Geophysical Institute of Peru (IGN) in the World Geodetic System WGS84/UTM Zone 19S.

## Hidrology

### Maximum precipitation thresholds

The thresholds are indicators that are related to the danger, be it precipitation, water level or flow. For a characterization of extreme rainfall (Table 1) a common criterion is to establish precipitation thresholds as climatic indices. The determination of maximum precipitation thresholds for this study was followed according to the procedure described by Alfaro (2014), which is used by technical standard in SENAMHI. The information base necessary to estimate the thresholds is the daily precipitation of a weather station with a long record, for this study the La Pampilla station was used, it is also mentioned that the use of these indices is justified because there is more information available from accumulated data of precipitation (daily rain) in 24 hours than precipitation intensities.





Check for updates

**Table 1.** Extreme rainfall differentiation.

Precipitation thresholds	Characterization of extreme rainfall
RR/día > 99p	Extremely Rainy
95p < RR/día ≤ 99p	Very rainy
90p < RR/día ≤ 95p	Rainy
75p < RR/día ≤ 90p	Moderately Rainy

\* RR/day is the accumulated amount of precipitation in 24 hours.

\*99p, 95p, 90p, 75p, are the percentiles expressed in %.

For the calculation of the percentiles, the procedure that must be taken into account is the following: 1) Exclude from the calculation the highest value of the series; 2) When "Outliers" are observed in the historical series, it is necessary to verify their impact on the statistical parameters of the series due to their presence; 3) Exclude from the calculation all days with traces; 4) Consider a day with precipitation when  $RR > 0.1$  mm; 5) If working with Excel, use the PERCENTIL.INC function; 6) If possible, use the reference period established by SENAMHI for climate characterization (1981 – 2010), if not, explicitly refer to the period analyzed; 7) The length of the series is very important since it affects the determination of the thresholds, therefore it is recommended to take as reference those stations where the data begin in 1981; 8) The length of the ideal series is the one established for climatic characterization, if it were not possible to do this, it is recommended that the reader be explicitly warned to be careful with the use of these results, and not consider them as climatic thresholds, but thresholds derived from the



sample used (it is suggested that samples not less than 10 years); 9) The results obtained must be carefully used if special extrapolations are intended, given the high spatial variability of rainfall; 10) For the use of the data, the quality of the data from the stations must be evaluated.

Thouret *et al.* (2013) provided mapping and cartography as a source of support for the hazard and risk of flash floods and lahars (volcanic mudflows) of the San Lázaro and Huarangal streams based on the morphology of the channels, however, it is required of a precipitation-runoff analysis to determine the maximum flows through a hydrological model based on observed data (La Pampilla Station). The delimitation of the basins (Figure 11) was carried out following the good practices developed in Qgis, by Van Der Kwast & Menke (2019), determining the physiographic and geomorphological characteristics for each study gorge based on the digital elevation model (DEM) ALOS-PALSAR, at a resolution of 12.5 m.

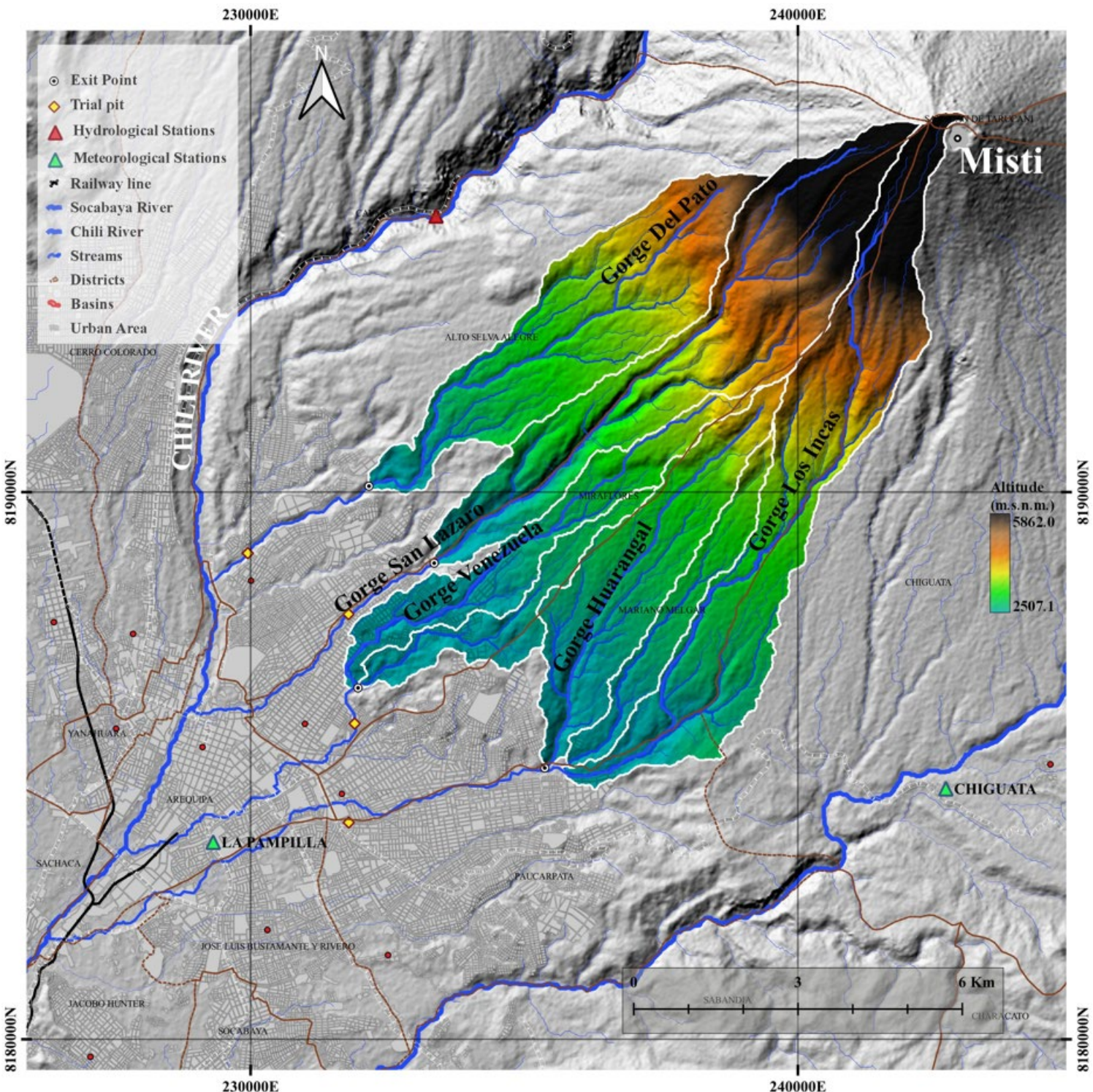


**Figure 11.** Delimitation of the studied drainage basin.

The liquid hydrograph was obtained from 24-hour maximum rainfall data from the stations: La Pampilla and Chiguata (Table 2), with a record of 41 years (1981-2021), ruling out the Huasacache station due to the area of influence over gullies, by the method of Thiessen polygons.

**Table 2.** Meteorological stations.

Meteorological stations	Longitude (°)	Latitude (°)	Altitude (masl)
La Pampilla Station	-71.534	-16.413	2 326
Chiguata Station	-71.409	-16.406	2 902

The frequency analysis was performed on the data through the non-parametric test of goodness and fit Smirnov-Kolmogorov with a significance level of  $\alpha=0.05$  with the Hydrognomon software, for different probability distribution functions and to know which one fits best to the maximum data series, the extreme value theory was taken into account to characterize extreme precipitation events as mentioned by Endara (2017), generalized extreme value (**GEV**) distribution. Then, to determine the hydrograph, the HEC-HMS hydrological model was used, with the Soil Conservation Service (SCS, 1986) methodology to know the net rainfall with the curve number (SCS, 1972) and the method of precipitation runoff transformation by unit hydrograph (SCS, 1972). For the present study, the SCS-Type II storm distribution was used, which calculates the flood hydrographs for 24-hour precipitation and the Type II distribution

because they are high Andean basins. The input parameters to the HEC-HMS model are those shown in Table 3.

**Table 3.** Parameters of the gorges of the study.

Basin	Basin Area (km <sup>2</sup> )	Medium Slope (%)	Curve Number (CN)	Concentration Time (Tc)
Del Pato	13.8	24.6	81.8	53.8
San Lázaro	17.0	42.8	84.4	52.0
Venezuela (i)	6.5	18.9	82.2	62.8
Venezuela (ii)	3.6	17.7	81.7	52.6
Los Incas (i)	9.8	18.4	81.7	53.5
Los Incas (ii)	4.0	16.5	81.7	49.2
Los Incas (iii)	17.8	30.1	83.5	67.3

\* Concentration time in minutes.

The gullies that are located on the left bank of the Chili River and that flow towards it, present a slope of the main channel between 7 to 18 % (Figure 12).



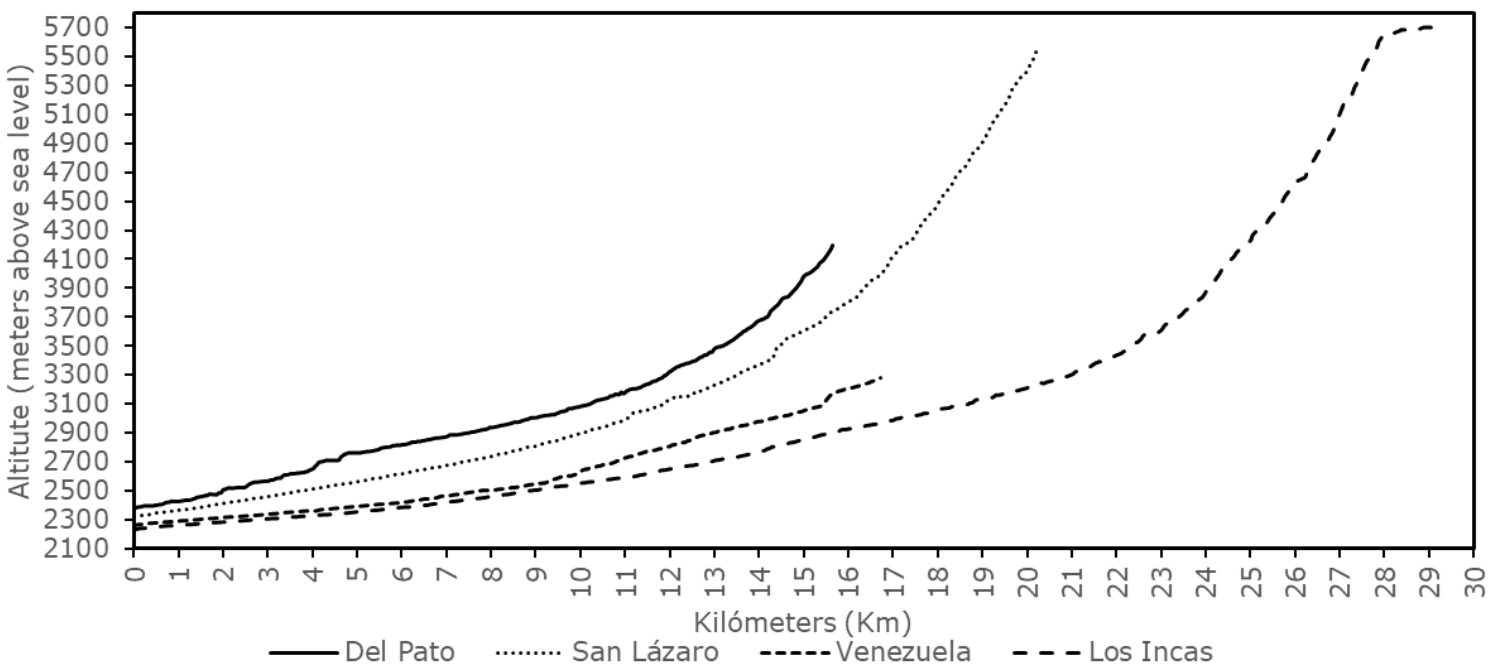


**Figure 12.** Longitudinal profile of the gorges until the confluence at Chili River.

Table 4 shows the liquid flows estimated with the HEC-HMS model for each study basin.

**Table 4.** Estimated maximum liquid flows.

Basin	Flow rate ( $\text{m}^3/\text{s}$ ) for different return periods (years)				
	TR = 5	TR = 25	TR = 50	TR = 100	TR = 200
Del Pato	7.0	24.9	34.7	45.3	56.3
San Lázaro	15.9	46.8	61.8	77.4	93.5
Venezuela	10.0	23.9	31.0	38.6	46.5
Los Incas	22.2	69.6	93.1	117.7	143.1

\*TR: Return Period.



## Soil mechanics

Samples were taken through test pits at critical points at the entrance to the city of Arequipa (Figure 11) for the different evaluated gullies according to the Peruvian Technical Standard (NTP), in this way the geotechnical characteristics were determined through laboratory tests such as the test method for granulometric analysis by sieving NTP 339.128, test to determine the relative specific weight of the solid particles of a soil NTP 339.131, test to determine the mass per unit volume or density (unit weight) NTP 400.017 and standard test for direct cutting of soils under consolidated drained conditions NTP 339.171 at a maximum depth of 1.5 m (Table 5). Where the sediment matrix is made up mainly of sand and gravel over the fines (less than 8 %), which suggests the null cohesion between the particles of sedimentary deposits, erodible soils, in the face of hyper-concentrated flows. The presence of flanks made up of mud flows, lahars and solid waste was also found.

**Table 5.** Summary of soil mechanics tests carried out.

Variable	Del Pato	San Lázaro	Venezuela	Los Incas
Depth (m)	1.5	1.5	1.5	1.5
Gravel (%)	34.6	43.8	33.7	22.0
Sand (%)	58.5	51.5	57.9	74.2
Fine aggregate (%)	6.9	4.7	8.4	3.8
D95 (mm)	35.6	60.0	55.2	40.0
D90 (mm)	24.6	52.4	43.4	19.3
D50 (mm)	1.0	3.0	1.6	0.5
SUCS	SM	GP	GP	GP
Moisture (%)	0.4	6.7	0.9	6.7
Unit weight (gr/cm <sup>3</sup> )	1.67	1.67	1.92	1.67
Specific gravity (G)	2.62	2.55	2.53	2.58
Internal friction angle (°)	33	35	33	33

\*SM (silty sands); GP (gravels with bad gradation).

## Hyperconcentrated flows

The mixture of sediments and water that flow in a channel, in Peru are known as "huaycos" (landslides, mudslides or debris flow) (Castillo, 2006). The record of floods and debris flows (huaycos) is common in semi-arid areas such as Arequipa, generally associated with intense rains that flow through the gorges later gullies that are born in the Misti volcano (Rivera, Vílchez, & Vela, 2018). Suárez (2001) shows longitudinal profiles



of channels for different types of flow (mud flows, hyperconcentrated flows and debris flows) where the direct relationship between the slope and the length of the main channel for each given event can be seen. According to the type of flow and the slope characteristics of the study gullies (Figure 12), the type of flow was characterized by the presence of mud during the event in the different gullies: San Lázaro (Fredysimplemente, 2012), Venezuela (El informativo AQP, 2020), Los Incas (El Búho pe, 2020) and landslide in the Del Pato gorge (INGEMMEN, 2019) through audiovisual reports as well as technical reports. Obtaining the hydrograph (Figure 13), represents the liquid part (precipitation), the solid part is represented by high concentrations of stones, gravel, sand and fines transported by the alluvial flow. To know this solid part, either in volume or in weight, O'Brien, Julien and Fullerton (1993) proceeded to determine the volumetric concentration of solids with rheological parameters estimated with empirical values given by Rickenman (1999), from 1 600 to 2 000 kg/m<sup>3</sup> for flows of mud or sludge (mud flow) and from 1 900 to 2 300 kg/m<sup>3</sup> for flows of "huaycos" (debris flow). In this way, to determine these volumetric concentrations of solids, the formulas proposed by Takahashi (1991) were applied (Equation (1)) assuming a stable flow in motion (Almeida, Quisca, & Castillo, 2019):

$$C_v = \frac{\gamma_b S}{(\gamma_s - \gamma_b)(\tan \phi - S)} \quad (1)$$

Where:

$\gamma_b$  = Specific weight of the mud (1.0-1.6 ton/m<sup>3</sup>)



$\gamma_s$  = Specific weight of solid material (2.6 ton/m<sup>3</sup>)

$S$  = Average slope of the stream bed

$\phi$  = Angle of internal friction of the solid material (30°-35°)

The maximum flow rate of mud with respect to the flow rate of water and material in suspension is Equation (2):

$$Q_b = \frac{\gamma_s - \gamma}{\gamma_s - \gamma_b} Q_1 \quad (2)$$

Where:

$\gamma$  = Specific weight of water (1.0 ton/m<sup>3</sup>)

$Q_1$  = Maximum flow of water (m<sup>3</sup>/s)

$Q_b$  = Maximum flow of mud (m<sup>3</sup>/s)

The maximum flow rate of mudslide in saturated condition results with Equation (3):

$$Q_h = \frac{C^*}{C^* - C_V} Q_1 \quad (3)$$

Where:

$C^*$  = Maximum concentration of solid material at rest (0.6)

Figure 13 shows the mudslide flow hydrograph for the El Pato gorge, built from the liquid or water flow hydrograph.



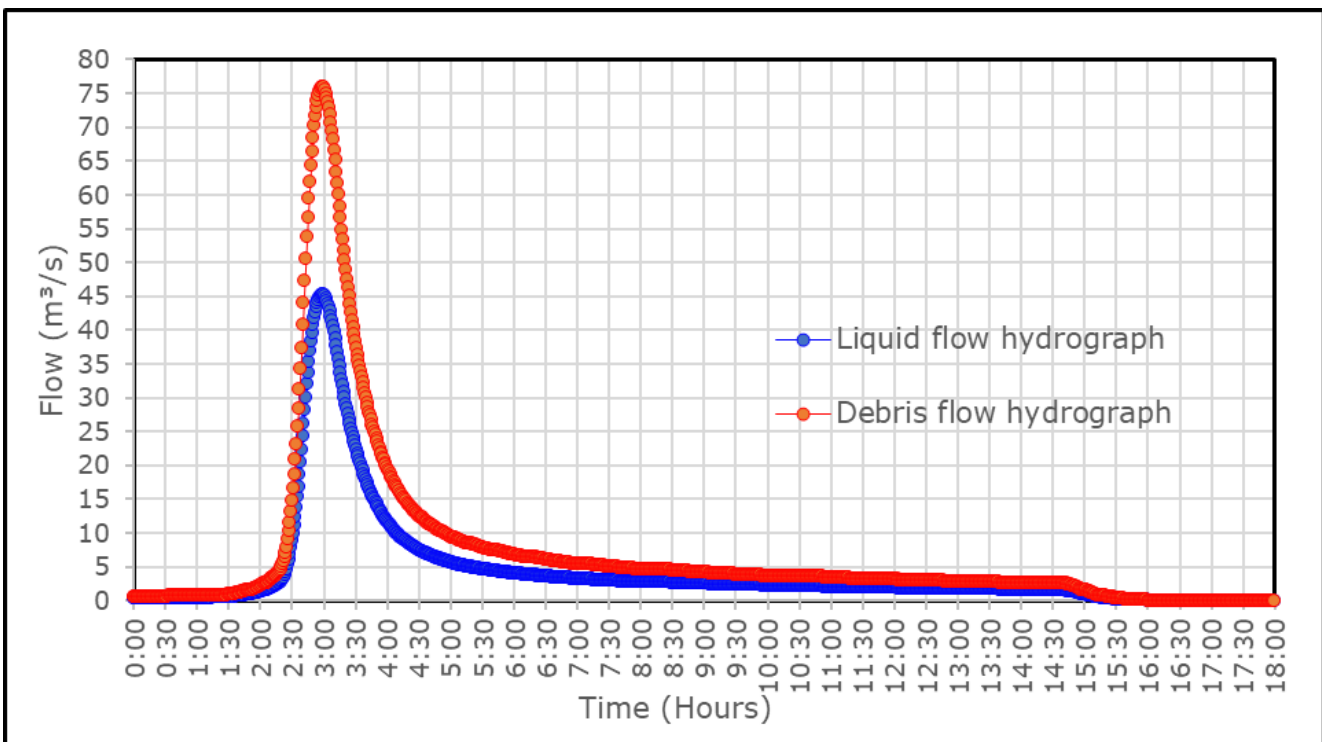


**Figure 13.** Liquid and debris flow Hydrograph of Del Pato gorge, TR = 100 years.

## Flood simulation

Determining flood hazard maps generally takes two steps, a hydrologic analysis to determine the magnitude of low-probability (100-year) storm discharge and a hydraulic model to estimate flow depth according to Mazer *et al.* (2021). In Peru, the ANA is a Public Organization attached to the Ministry of Agriculture and Irrigation, responsible for issuing standards and establishing procedures for the integrated and sustainable management of water resources. In this way, guarantee the protection, primary use of water, free transit, fishing, etc. With the purpose of establishing an upper limit of the riverbank, a Marginal Strip, where it is

indicated that in lands adjacent to the natural or artificial channels of the water sources adjacent to population settlements, a return period of 100 years, according to the Use and Management of Marginal Belts (ANA, 2020).

The flood analysis for each gully was carried out with the help of the HEC-RAS (Hydrological Engineering Center-River Analysis System) software, taking into account the boundary or border conditions of the entrance (Flow Hydrograph), exit (Normal Depth) and roughness of Manning (Figure 14), taking values recommended by the hydraulic book of open channels by Ven Te Chow (1994).



**Figure 14.** Manning's coefficient in the different evaluated gullies: A) Del Pato, B) San Lázaro, C) Venezuela and D) Los Incas.

The flood simulation was carried out under the analysis of non-permanent or non-steady flow that solves in a two-dimensional differential way the free surface flow (Equation (4)) for the calculation of the depth and the speed of water in the "x" and "y" axes. This equation represents the expression of the physical principle of conservation of liquid mass in a fluid, in its conservative (fixed control volume) and differential form (Anderson, 1995):

$$\frac{\partial h}{\partial t} + \frac{\partial(hu)}{\partial x} + \frac{\partial(hv)}{\partial y} = 0 \quad (4)$$

Where:

$h$  = Flow depth

$u$  = Velocity in axis "x"

$v$  = Velocity in axis "y"

$t$  = Time

From Equation (4), which is the general equation of two-dimensional free surface flow, the HEC-RAS numerical model adds a variable "q" (infiltration) (Equation (5)) that will not be taken into account in this study because they are maximum values. avenues.

Equation of continuity of two-dimensional flow in free surface:



$$\frac{\partial H}{\partial t} + h \frac{\partial(u)}{\partial x} + h \frac{\partial(v)}{\partial y} + q = 0 \quad (5)$$

Momentum equation of two-dimensional flow in free surface in the "x" and "y" axis (equations (6) and (7)):

$$\frac{\partial u}{\partial t} + u \frac{\partial u}{\partial x} + v \frac{\partial u}{\partial y} = -g \frac{\partial H}{\partial x} + u_t \left( \frac{\partial^2 u}{\partial x^2} + \frac{\partial^2 u}{\partial y^2} \right) - c_f u + f v \quad (6)$$

$$\frac{\partial v}{\partial t} + u \frac{\partial v}{\partial x} + v \frac{\partial v}{\partial y} = -g \frac{\partial H}{\partial y} + u_t \left( \frac{\partial^2 v}{\partial x^2} + \frac{\partial^2 v}{\partial y^2} \right) - c_f v + f u \quad (7)$$

Where:

$H$  = Elevation of the surface of water

$u$  = Velocity in axis "x"

$v$  = Velocity in axis "y"

$t$  = Time

$c_f$  = Resistance coefficient

$f$  = Coriolis parameter



## Model calibration

The calibration was carried out taking into account the maximum rainfall records (1981-2021) that triggered historical events in the city of Arequipa: 1995, 1997, 2001, 2002, 2012, 2015, 2016 and 2020, as an adverse meteorological phenomenon, understood in statistical terms as less likely. Cruz (2009) analyzed the event of February 25, 1997 in the Huarangal torrent that generated the flood, one of the most dramatic in a long time. Martelli (2011) summarized nine events that caused damage to the city of Arequipa based on recurring flood scenarios from 5 to 10 years. However, the calibration of the hydraulic model was carried out for a return period of TR=5 years, according to the analysis of precipitation thresholds with the indicator of extremely rainy through historical events that have occurred in the city of Arequipa, affecting the infrastructures present in the riverbeds from an engineering point of view. The streams studied are characterized by being dry for almost the entire year, since they are only activated in periods of high intensity rain or the occurrence of extreme hydrological events, as was the case in 2020, a common denominator in the level of water level under the existing infrastructures (Figure 15) in the lined canalized channels.

(A)



(B)



(C)



(D)



**Figure 15.** Existing infrastructures in the bed of the different gullies: A) Del Pato Gully (Puente s/n); B) San Lázaro Gully (Av. Juan de la Torre); C) Venezuela Gully (El Palomar); D) Los Incas Gully (land terminal).

## Results

For the La Pampilla Station, the accumulated precipitation data was ordered from the lowest to the highest 932 days with rain ( $RR > 0.1\text{mm}$ ) and the percentiles of the series of 931 days with rain were calculated, excluding the highest value recorded (124.5 mm) due to exceptional rain (Cacya, Meza, Carlotto, & Mamani, 2013), and the statistics of extreme values (Table 6 and Table 7). There were 273 missing data in the series (Figure 16).

**Table 6.** Historical record.

Meteorological Stations	Period	Number of years	Missing data (%)
La Pampilla Station	1981-2021	41	5.4
Chiguata Station	1981-2021	41	5.7

\* Information on maximum daily precipitation was collected from SENAMHI.

**Table 7.** Maximum precipitation thresholds for the La Pampilla station.

Precipitation Thresholds	Characterization of extreme rainfall
$RR/\text{día} > 99 \text{ p}$	$RR > 25.5 \text{ mm}$
$95 \text{ p} < RR/\text{día} \leq 99 \text{ p}$	$14.6 \text{ mm} < RR \leq 25.5 \text{ mm}$
$90 \text{ p} < RR/\text{día} \leq 95 \text{ p}$	$10.2 \text{ mm} < RR \leq 14.6 \text{ mm}$
$75 \text{ p} < RR/\text{día} \leq 90 \text{ p}$	$4.5 \text{ mm} < RR \leq 10.2 \text{ mm}$



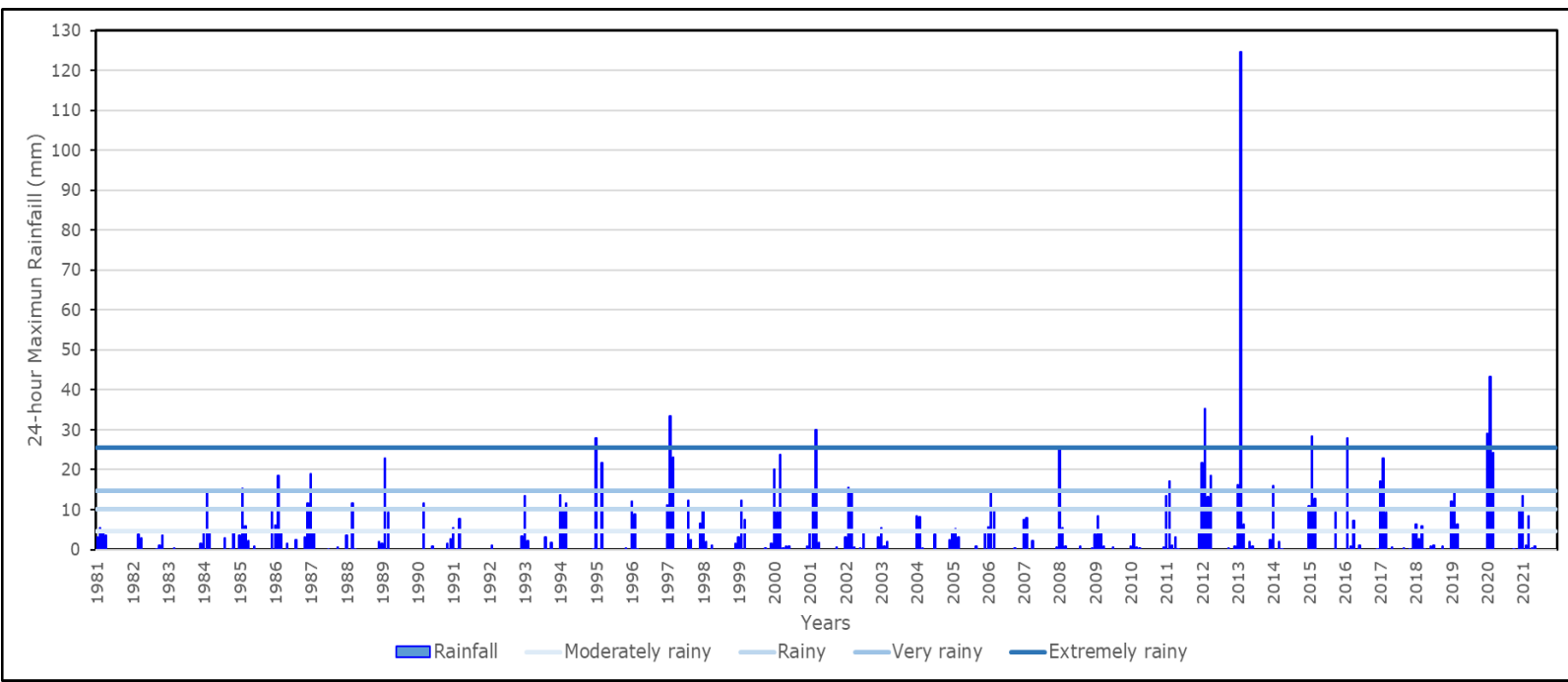


**Figure 16.** La Pampilla Station (1981-2021)-Daily maximum precipitation data.

The treatment of maximum precipitation data of 24 hours responds well to the expected behavior of the precipitation of the La Pampilla station through the use of percentiles (Figure 17).

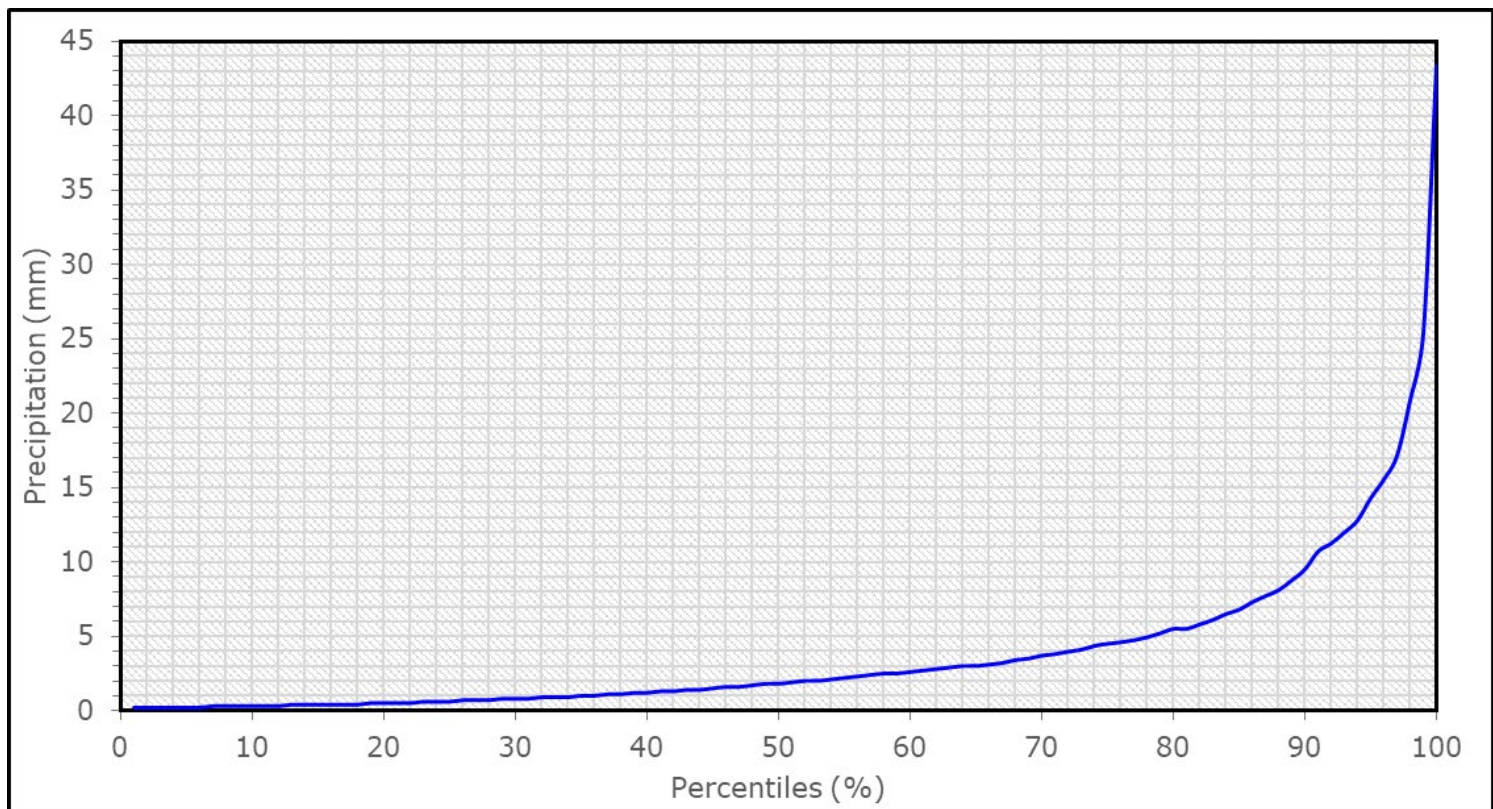


**Figure 17.** La Pampilla Station (1981-2021), precipitation in (mm) vs. percentiles (%).

Table 8 shows the flows determined according to the type of flow under analysis.

**Table 8.** Maximum flows for different return periods (TR).

Gorge	Maximum flow (m³/s)	Cd	Flow (m³/s) for different return periods (years)				
			TR = 5	TR = 25	TR = 50	TR = 100	TR = 200
<b>Del Pato</b>	Water Flow	-	7.0	24.9	34.7	45.3	56.4
	Mud Flow	1.23	8.6	30.6	42.7	55.7	69.4
	<b>Debris flow (Takahashi formula)</b>	<b>1.68</b>	<b>11.7</b>	<b>41.8</b>	<b>58.2</b>	<b>76.0</b>	<b>94.6</b>
<b>San Lázaro</b>	Water flow	-	15.9	46.8	61.8	77.4	93.5
	<b>Mud flow</b>	<b>1.14</b>	<b>18.2</b>	<b>53.5</b>	<b>70.6</b>	<b>88.5</b>	<b>106.9</b>
	Debris flow (Takahashi formula)	2.44	38.7	114.0	150.5	188.5	227.8
<b>Venezuela</b>	Water Flow	-	10.0	23.9	31.0	38.6	46.5
	<b>Mud Flow</b>	<b>1.14</b>	<b>11.4</b>	<b>27.3</b>	<b>35.4</b>	<b>44.1</b>	<b>53.1</b>
	Debris flow (Takahashi formula)	1.21	12.1	28.9	37.5	46.7	56.2
<b>Los Incas</b>	Water Flow	-	22.2	69.6	93.1	117.7	143.1
	<b>Mud Flow</b>	<b>1.14</b>	<b>25.4</b>	<b>79.6</b>	<b>106.4</b>	<b>134.5</b>	<b>163.6</b>
	Debris flow (Takahashi formula)	1.52	33.8	106.1	141.9	179.4	218.1

\*Cd: Thickening factor.

Figure 18, Figure 19, Figure 20 and Figure 21 show maps by flood hazard.



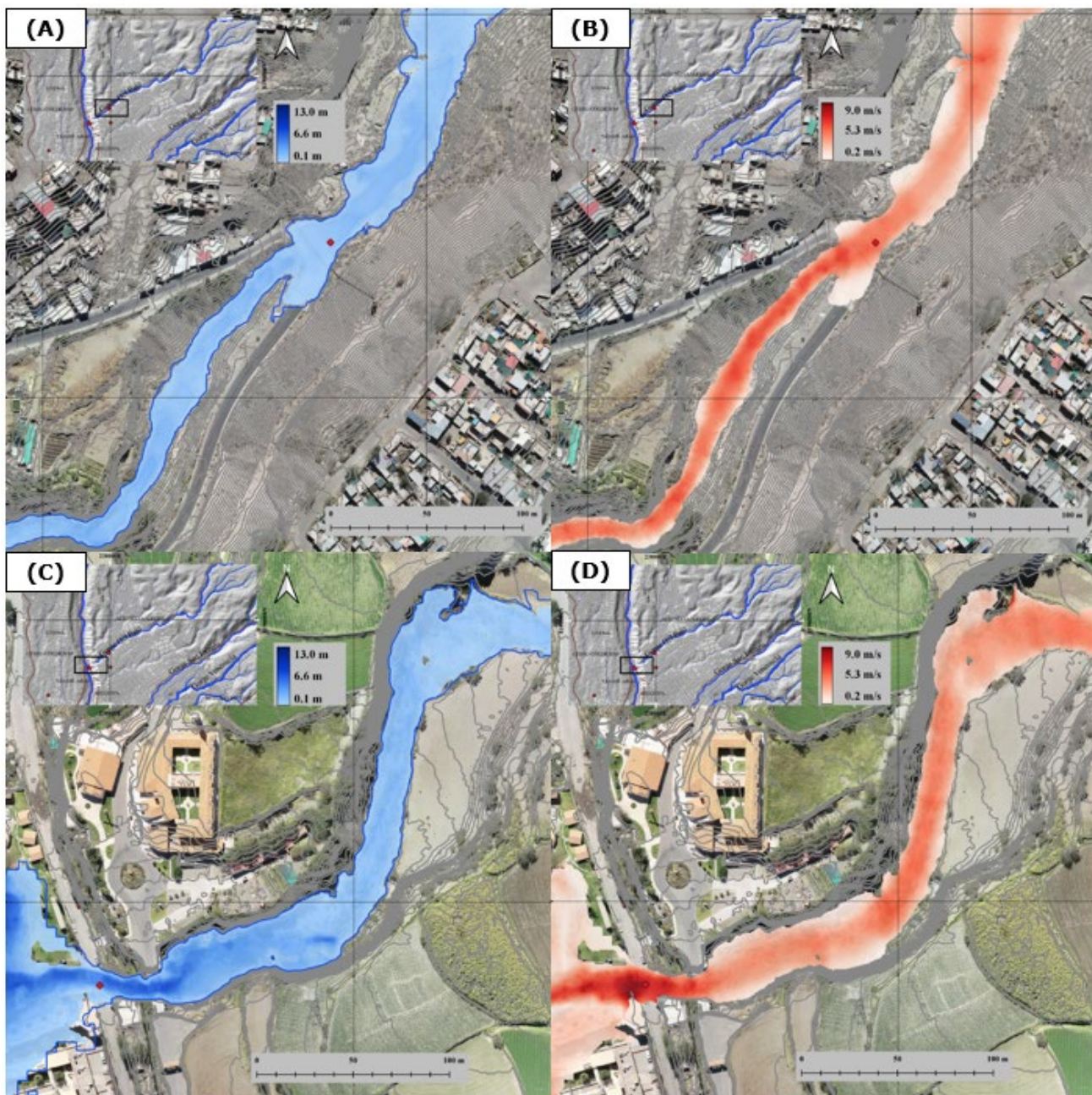


**Figure 18.** Flood hazard map, for a return period of 100 years A), B) water depth and velocities in the existing dip; C), D) water depth and velocities in the unnamed bridge of the Del Pato gully, using the HEC-RAS numerical model.



**Figure 19.** Flood hazard map, for a return period of 100 years A), B) water depth and speeds on the Cahuide bridge; C), D) water depth and velocities in Av. Juan de la Torre of the San Lázaro gully, using the HEC-RAS numerical model.



**Figure 20.** Flood hazard map, for a return period of 100 years A), B) water depth and speeds on Av. C18/Santa Rita Bridge; C), D) water depth and speeds on the Venezuela gully railway bridge, using the HEC-RAS numerical model.

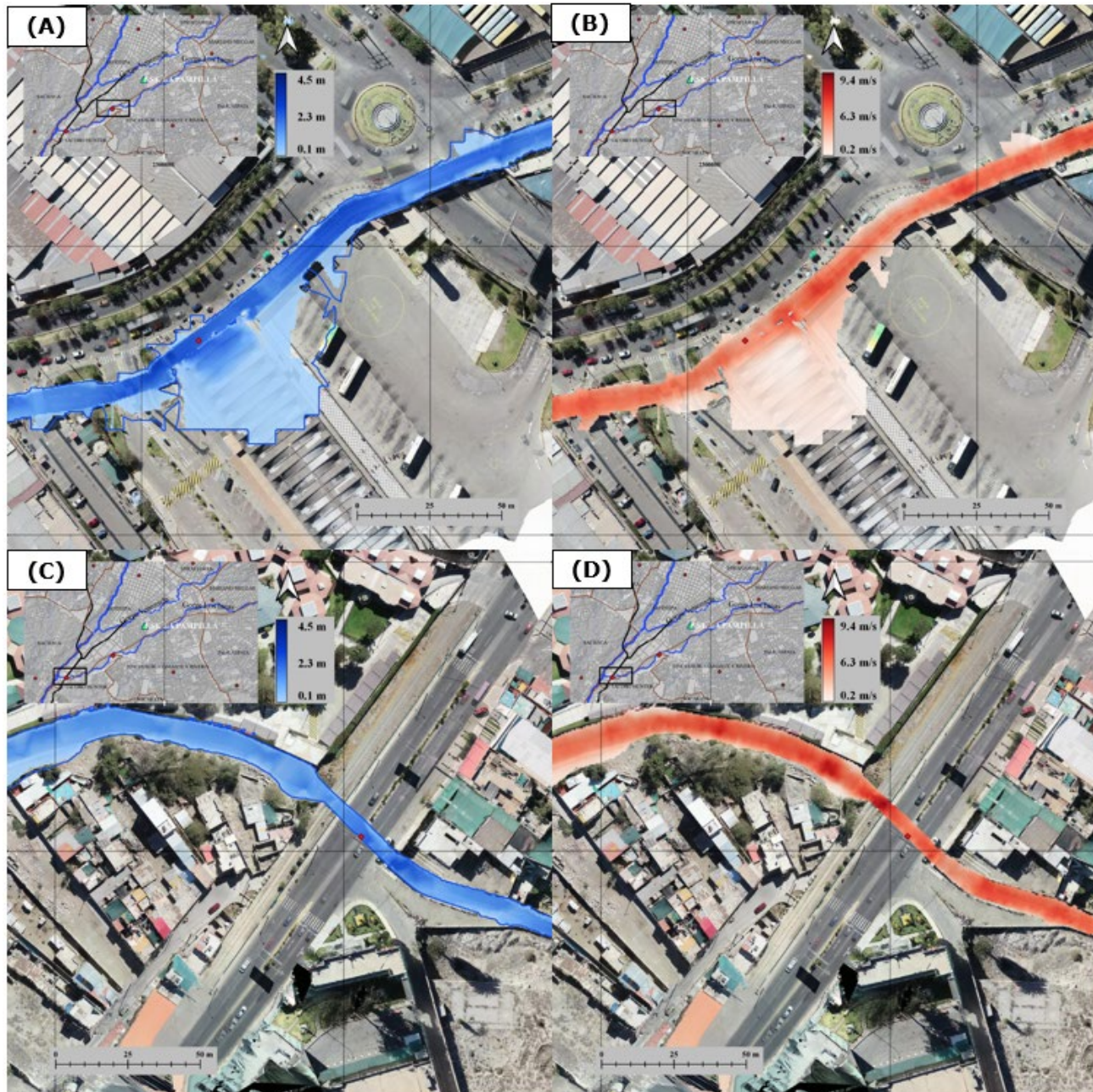


**Figure 21.** Flood hazard map, for a return period of 100 years A), B) depth of water and speeds of the Bus Terminal and Terrapuerto; C), D) water depth and velocities on the Av. Alfonso Ugarte bridge of the Los Incas torrentera, using the HEC-RAS numerical model.

The evaluation in the field and the main hydraulic parameters through the numerical simulations (Table 9), show historical events, danger points and risk zones in front of maximum avenues.

**Table 9.** Evaluation of results for disaster risk management.

Gullies of the study	Risk area/infrastructure	Frequency of events (Years)	Return period (TR)	Maximum water depth (m)	Maximum flow speed (m/s)	Total flooded área (ha)
<b>Del Pato gully (9.3 km)</b>	Existing gully	High (every 3 to 5 years)	100	0.9	5.4	20.3
	NN Bridge		100	5.8	5.1	
<b>San Lázaro gully (8.5 km)</b>	Cahuide bridge	High (every 3 to 5 years)	100	4.8	6.3	23.4
	Juan de la Torre Ave.		100	5.1	6.2	
<b>Venezuela gully (6.7 km)</b>	C18 Ave, Santa Rita bridge	High (every 3 to 5 years)	100	3.6	2.2	7.7
	Train bridge		100	1.7	3.0	
<b>Los Incas gully (6.9 km)</b>	Terminal Terrestre and Terrapuerto	High (every 3 to 5 years)	100	2.9	4.8	8.6
	Alfonso Ugarte Ave. bridge		100	2.4	6.0	



## Discussion

This study proposes the thresholds of maximum precipitation (extreme rainfall) as an early warning system (Figure 15) that, instead of deducing the probability density function, estimates the thresholds of extreme precipitation events by means of an empirical probability function, characterized with "extremely rainy" rainfall greater than 25.5 mm, which triggers landslides and rockfalls (Figure 22), in the lined and natural canalized channels of the different study streams (Del Pato, San Lázaro, Venezuela and Los Incas) from the city of Arequipa.



**Figure 22.** Heavy rains trigger erosion and undermining of the San Lázaro gorge.

The gullies are straight and steep channels, dominated by a one-dimensional flow (1D) Bricker *et al.* (2017). The existing infrastructures such as bridges and pontoons within the gullies of the city of Arequipa were configured under these criteria, through cross sections, taking into account the coefficients of expansion (0.5), contraction (0.3) and the contour conditions or of border (Normal Depth) for a 1D model, in this way, to know the depth/flow height at the lower level of the deck of the infrastructures present by water footprint (Figure 13) to later model under a two-dimensional (2D) flow approach with HEC-RAS, which solve the Saint-Venant two-dimensional differential equations with the Finite Volumes method, with a cell size of 5x5 meters and a computational time interval of three seconds.

The occurrence of rains occurs in the upper part (gorge), middle and lower part (gorge) or simultaneously, the flow of water at the point of exit (Figure 11), arrives with a high load of sediments, which rheologically constitute hyperconcentrated flows, mud or mud flow and landslides, presence of solids of extended granulometry (stones and/or rocks) as shown by the study of soil mechanics (Table 5) and that according to the longitudinal profiles of the streams studied (Figure 12 ) with a maximum of 18 %, the direct relationship between the slope of the main channel with the taxonomy of non-Newtonian flows is seen through a thickening factor of the liquid hydrograph, by the formulation described by Takahashi (1991).

The results (maximum flows) values obtained with the empirical formulation of Takahashi are reasonable and consistent with the traces

left in historical events that occurred in the gullies of study as it was in the year 2020, from an engineering point of view for decision-making in the face of danger by floods. However, it is recommended to carry out the analysis for mud and debris flows (landslides) with the taxonomy proposed by Gibson, Floyd, Sánchez and Heath (2020) using Bingham and O'Brien Equation (Quadratic) rheological models for a better understanding of not newtonian flows.

It is recommended to add milestones by the National Water Authority (ANA) in the upper parts of the gorges through marginal strips, to promote an education tool for the population, about the dangers of settling in border areas banks of riverbeds in the face of extreme events and the different government entities (Municipalities and Regional Government) for adequate territorial planning.

This research allowed, in an unprecedented way, to quantify the areas of danger due to floods in the city of Arequipa. The applied methodology can serve as a basis for solving similar problems in other cities through the importance of disaster risk management in the face of climate change.

## Conclusions

The characterization of the maximum rainfall of 24 hours (extreme rainfall) of the La Pampilla station between 1981-2021 (14,975 data) allowed to determine an "extremely rainy" threshold (99th percentile) that occurs approximately every 5 years in the city of Arequipa as events

triggering rapid mass movements such as the years 1995, 1997, 2001, 2008, 2012, 2013, 2015, 2016 and 2020.

The evaluated gorges (Del Pato, San Lázaro, Venezuela and Los Incas) are made up mainly of alluvial deposits, made up of sand, gravel and fines. Also presenting mud flow flanks and lahars that are highly erodible by hyper-concentrated flows.

The frequency analysis of the maximum 24-hour rainfall of the La Pampilla station was carried out, the results of the probabilistic model, Generalized Extreme Value (GEV), have been chosen, since according to the goodness of fit test Smirnov-Kolmogorov with a level of significance of  $\alpha = 0.05$ , such probability distribution satisfactorily fits the data of the sample, with a record of 41 years (1981-2021).

The flood hydrographs of the study streams were estimated with the HEC-HMS numerical model, taking into account a hypothetical storm meteorological model, by the SCS Type II method developed by the U.S. Soil Conservation Service (US-SCS) for 24-hour rainfall applicable to high Andean basins. The calibration of the model was carried out taking into account the records of historical events raised in the city of Arequipa (1981-2021) through the analysis of maximum precipitation thresholds.

The flow transit (flood simulation) was carried out with the HEC-RAS numerical model, for a return period of 100 years, because they are areas adjacent to population settlements, according to the Use and Management of Marginal Strips dictated by the National Authority. of Water (ANA).

The results show flow depths and critical velocities, producing scour and erosion in the channels under analysis, as well as overflow and



flooding areas caused by extreme rainfall that are becoming more frequent, thus taking responses to the high risk for the city of Arequipa, such as staggered falls (energy dissipation), shim work on bridge abutments and retaining walls.

### Acknowledgment

To the Catholic University of Santa María for the funding through which this research project was developed.

### References

- Anderson, J. (1995). Computational fluid dynamics: The basics with applications. New York, USA: McGraw-Hill.
- Alfaro, L. (2014). Estimación de umbrales de precipitación extremas para la emisión de avisos meteorológicos (Nota Técnica 001). Recovered from <https://hdl.handle.net/20.500.12542/345>
- Almeida, A., Quisca, S., & Castillo, L. (2019). Numerical simulation of debris flows of the catastrophic event of February 2019 in Mirave-Peru. DOI: 10.4136/ambi-agua.2437
- ANA, Autoridad Nacional del Agua. (2015). Plan de gestión de los recursos hídricos de la cuenca Quilca-Chili. Recovered from <https://hdl.handle.net/20.500.12543/86>
- ANA, Autoridad Nacional del Agua. (2016). Priorización de cuencas para la gestión de los recursos hídricos. Recovered from <https://hdl.handle.net/20.500.12543/205>

ANA, Autoridad Nacional del Agua. (2020). Uso y gestión de fajas marginales. Recovered from <https://hdl.handle.net/20.500.12543/4636>

Bricker, J. D., Schwanghart, W., Adhikari, B. R., Moriguchi, S., Roeber, V., & Giri, S. (2017). Performance of models for flash flood warning and hazard assessment: The 2015 Kali Gandaki landslide dam breach in Nepal. *Mountain Research and Development*, 37(1), 5-15. DOI: 10.1659/MRD-JOURNAL-D-16-00043.1

Cacya, L., Meza, P., Carlotto, V., & Mamani, L. (2013). Aluvión del 8 de febrero del 2013 en la ciudad de Arequipa. En: Foro Internacional Peligros Geológicos (pp. 195-200). Arequipa, Perú: Instituto Geológico, Minero y Metalúrgico. Recovered from <https://hdl.handle.net/20.500.12544/1132>

Castillo, L. (2006). Aplicación de un modelo numérico de flujo de escombros y lodo en una quebrada en el Perú. Lima, Perú: Universidad Nacional de Ingeniería.

Chow, V. T. (1994). Hidráulica de canales abiertos. Santa Fe de Bogotá, Colombia: McGraw-Hill.

Clima y Ecología de Arequipa. (22 de febrero, 2013). Los desastres de 1989 y 2013: una sola fecha, 8 de febrero. Clima y Ecología de Arequipa. Recovered from <http://ecoclimaqp.blogspot.com/2013/02/los-desastres-de-1989-y-2013-una-sola.html>

Cruz, R. (2009). Gestión del riesgo por inundación en asentamientos populares, distrito de Mariano Melgar, Arequipa. Arequipa, Perú: Instituto Nacional de Defensa Civil.

Diario Correo. (8 de febrero, 2014). El aluvión del 8 de febrero. Diario Correo. Recovered from <https://diariocorreo.pe/peru/el-aluvion-del-8-de-febrero-fotos-51126/>

Endara, S. (diciembre, 2017). Determinación de extremos de precipitación a partir del PISCO diario. Lima, Perú: Servicio Nacional de Meteorología e Hidrología del Perú, Dirección de Hidrología. Recovered from <https://hdl.handle.net/20.500.12542/955>

El Búho. (29 de febrero, 2015a). Represas al 70% de su capacidad de almacenamiento tras recientes lluvias. El Búho. Recovered from <https://elbuho.pe/2016/02/represas-al-70-de-su-capacidad-de-almacenamiento-tras-recientes-lluvias/>

El Búho. (2 de febrero, 2015b, c). Lluvias ponen al descubierto precariedad de “obras” viales. El Búho. Recovered from <https://elbuho.pe/archivo/2015/02/02/lluvias-ponen-al-descubierto-precariedad-de-obras-viales/index.html>

El Búho. (23 de febrero, 2016a). Lluvia de 10 horas y apagón afectaron la ciudad de Arequipa. El Búho. Recovered from <https://elbuho.pe/2016/02/fotos-lluvia-de-10-horas-y-apagon-afectaron-la-ciudad-de-arequipa/>

El Búho. (24 de febrero, 2016b). Más de 3,500 familias y 10 mil metros de vías afectadas por las lluvias de dos días. El Búho. Recovered from <https://elbuho.pe/2016/02/mariano-melgar-yura-y-alto-selva-alegre-fueron-los-distritos-mas-afectados-por-lluvias/>

El Búho. (8 de marzo, 2017a). Disminuyen caudal que vierte a torrentera Chullo para reparar puente La Concordia. El Búho. Recovered from <https://elbuho.pe/archivo/2017/03/08/disminuyen-caudal-que-vierte-a-torrentera-chullo-para-reparar-puente-la-concordia/index.html>

El Búho. (30 de enero, 2017b). Otra víctima mortal cobró el huaico que ingresó por torrentera de Paucarpata. El Búho. Recovered from <https://elbuho.pe/archivo/2017/01/30/otra-victima-mortal-cobro-el-huaico-que-ingreso-por-torrentera-de-paucarpata/index.html>

El Búho. (26 de febrero, 2020a). Pronóstico: lluvias fuertes continuarán en Arequipa, advierte Senamhi. El Búho. Recovered from <https://elbuho.pe/2020/02/hoy-continuaran-las-lluvias-fuertes-en-arequipa/>

El Búho. (26 de febrero, 2020b). Lluvias en Arequipa: más de 250 viviendas afectadas por desbordes e inundaciones. El Búho. Recovered from <https://elbuho.pe/2020/02/lluvias-en-arequipa-mas-de-250-viviendas-afectadas-por-desbordes-e-inundaciones/>

El Búho. (25 de febrero, 2020c). Lluvias en Arequipa: desborde de torrenteras en La Isla, Terminal Terrestre y Paucarpata. El Búho. Recovered from <https://elbuho.pe/2020/02/lluvias-en-arequipa-desborde-de-torrenteras-en-la-isla-terminal-terrestre-y-paucarpata/>

El Búho. (25 de febrero, 2020d). Terminales terrestres de Arequipa vuelven a reabrir después del ingreso de huaico. El Búho. Recovered from <https://elbuho.pe/2020/02/suspenden-salida-de-buses-de-arequipa-por-inundacion-de-terminales-terrestres/>

El Búho pe. (25 de febrero, 2020). Desborde de torrenteras en Arequipa. Recovered from <https://www.youtube.com/watch?v=0XAtMwZnPtM&t=18s>

El Búho. (28 de marzo, 2021). Hace 20 años el problema de las torrenteras y alcantarillado pluvial en Arequipa. El Búho. Recovered from <https://elbuho.pe/2021/03/hace20anos-el-problema-de-las-torrenteras-y-alcantarillado-pluvial-en-arequipa/>

El Informativo AQP. (29 de enero, 2020). Ingreso de la torrentera de la av. Venezuela en el Cercado de Arequipa. Recovered from [https://www.youtube.com/shorts/FHsQLvO\\_HNo](https://www.youtube.com/shorts/FHsQLvO_HNo)

Espinoza-Vigil, A. J., & Booker, J. D. (2023a). Building national disaster resilience: Assessment of ENSO-driven disasters in Peru. *International Journal of Disaster Resilience in the Built Environment*. DOI: 10.1108/IJDRBE-10-2022-0102

Espinoza-Vigil, A. J., & Booker, J. D. (2023b). Hydrological vulnerability assessment of riverine bridges: The Bajo Grau bridge case study. *Water*, 15(5), 846. DOI: 10.3390/w15050846

Ettinger, S., Mounaudb, L., Magill, C., Lafourcade, A. F., Thouret J. C., Manville, V., Negulescu C., Zuccaro G., De Gregorio, D., Nardone, S., Uchuchoque, J. A., Arguedas, A., Macedo, L., & Manrique, N. (2015). Building vulnerability to hydro-geomorphic hazards: Estimating damage probability from qualitative vulnerability assessment using logistic regression. *Journal of Hydrology*, 541(2016), 563-581. DOI: 10.1016/j.jhydrol.2015.04.017

Fredysimplemente. (Marzo, 2012). Huayco en torrentera San Lázaro Arequipa. Recovered from <https://www.youtube.com/watch?v=GAfRMaXJNdA>

Gestión. (14 de febrero, 2013). Arequipa: las pérdidas por inundaciones podrían superar los S/.350 millones. Recovered from <https://gestion.pe/economia/arequipa-perdidas-inundaciones-superar-s-350-millones-31633-noticia/?ref=gesr>

Gibson, S., Floyd, I., Sánchez, A., & Heath, R. (2020). Comparing single-phase, non-Newtonian approaches with experimental results: Validating flume-scale mud and debris flows in HEC-RAS. *Earth Surface Processes and Landforms*, 46, 540-553. DOI: 10.1002/esp.5044

INGEMMET, Instituto Geológico Minero y Metalúrgico. (2019). Evaluación de peligros geológicos en la quebrada El Pato, tramo Villa Confraternidad (zonas A, B, C y D). Región Arequipa, provincia Arequipa, distrito Alto Selva Alegre. Recovered from <https://hdl.handle.net/20.500.12544/2233>

INEI, Instituto Nacional de Estadística e Informática. (2017). Arequipa alberga a 1 millón 301 mil habitantes a los 476 años de su creación.

Nota de prensa. Recovered from <https://m.inei.gob.pe/prensa/noticias/arequipa-alberga-a-1-millon-301-mil-habitantes-a-los-476-anos-de-su-creacion-politica-9246/>

IPCC, The Intergovernmental Panel on Climate Change. (2022). Working group II contribution to the sixth assessment report of the intergovernmental panel on Climate Change Impacts, Adaptation and Vulnerability. Fact sheet – Central and South America. Geneva, Switzerland: The Intergovernmental Panel on Climate Change.

Martelli, K. (2011). The physical vulnerability of urban areas facing the threat of inundation from lahars and flash floods: Application to the case study of Arequipa, Peru. Recovered from [https://catalogobiblioteca.ingemmet.gob.pe/cgi-bin/koha/opac-detail.pl?biblionumber=46537&query\\_desc=an%3A1062%20and%20su-geo%3APERU](https://catalogobiblioteca.ingemmet.gob.pe/cgi-bin/koha/opac-detail.pl?biblionumber=46537&query_desc=an%3A1062%20and%20su-geo%3APERU)

Mazer, K., Tomasek, A., Daneshvar, F., Bowling, L., Frankenberger, J., McMillan, S., Novoa, H., & Zaballos, C. (2021). Integrated hydrologic and hydraulic analysis of torrential flood hazard in Arequipa, Peru. DOI: 10.1111/j.1936-704X.2020.3347.x

MINAM, Ministerio del Ambiente. (2018). Mapa de geología a nivel meso de la zonificación ecológica económica, región Arequipa. Recovered from <https://geoservidor.minam.gob.pe/zee-aprobadas/arequipa/>

Naciones Unidas. (2014). Manual para la evaluación de desastres.

Recovered from <https://www.cepal.org/es/publicaciones/35894-manual-la-evaluacion-desastres>

O'Brien, J., Julien, P., & Fullerton, W. T. (1993). Two-dimensional water flood and mudflow simulation. *Journal of Hydrologic Engineering*, ASCE. DOI: 10.1061/(ASCE)0733-9429(1993)119:2(244).1993

Rickenmann, D. (1999). Empirical relationships for debris flows. *Natural Hazards*, 19, 47-77. DOI: 10.1023/A:1008064220727

Rivera, M., Vílchez, M., & Vela, J. (2018). Peligros por huaycos en la ciudad de Arequipa. En: Taller Internacional Fortalecimiento de Capacidades para Mitigar los Impactos de Huaycos en Perú, Lima y Arequipa, Perú, 15-19 de octubre 2018. Libro de Resúmenes (pp. 45-49). Arequipa, Perú: Instituto Geológico, Minero y Metalúrgico. Recovered from <https://hdl.handle.net/20.500.12544/2589>

SENAMHI, Servicio Nacional de Meteorología e Hidrología del Perú. (2021). Climas del Perú: mapa de clasificación climática nacional. Recovered from <https://hdl.handle.net/20.500.12542/1336>

SCS, Soil Conservation Service. (1986). Urban hydrology for small watersheds. Technical Release No. 55 (TR-55). Washington, DC, USA: Department of Agriculture.

SCS, Soil Conservation Service. (1972). National engineering handbook. Section 4. Hydrology. Washington, DC, USA: U.S. Department of Agriculture.

Suárez, J. (2001). Control de erosión en zonas tropicales. Bucaramanga, Colombia: Instituto de Investigaciones sobre Erosión y Deslizamientos.

Takahashi, T. (1991). Debris Flow-IAHR Monograph Series. Rotterdam, The Netherlands: Balkema Publishers.

Thouret, J.-C., Enjolras, G., Martelli, K., Santoni, O., Luque, J. A., Nagata, M., Arguedas, A., & Macedo, L. (2013). Combining criteria for delineating lahar- and flash-flood-prone hazard and risk zones for the city of Arequipa, Peru. *Natural Hazards and Earth System Sciences*, 13, 339-360. DOI: 10.5194/nhess-13-339-2013

Van Der Kwast, H., & Menke, K. (2019). QGIS for hydrological applications recipes for catchment hydrology and water management. Recovered from <https://www.amazon.com.mx/QGIS-Hydrological-Applications-Catchment-Management/dp/0998547786>

Vílchez, M., & Sosa, N. (2021). Peligro geológico por movimientos en masa en la ciudad de Arequipa. Recovered from <https://hdl.handle.net/20.500.12544/3186>

Villalobos. (9 de febrero, 2012). Puente Grau. Villalobos. Recovered from <https://www.flickr.com/photos/dannyvf/6849722249/in/photostream/>

World Economic Forum. (2023). The global risks report. Geneva, Switzerland: World Economic Forum.